Signal Reconstruction from Modulo Observations

Viraj Shah

March 28, 2022

UIUC

In collaboration with Dr. Chinmay Hegde at Iowa State University
This work has been presented at GlobalSIP 2019.
An extended version is submitted to EURASIP.

Need for High Dynamic Range (HDR)

Signal acquisition

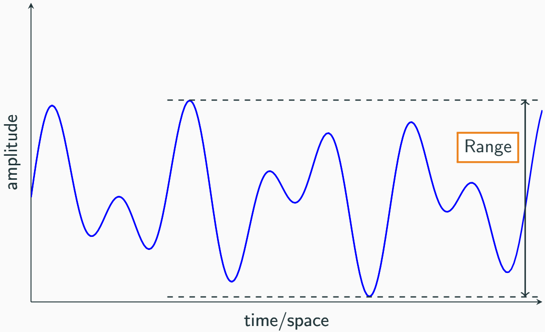

Imaging systems

- The Dynamic Range of the real signals can be very large.
- Dynamic range of the sensor is limited due to hardware constraint.

Need for High Dynamic Range (HDR)

Signal acquisition

Imaging systems

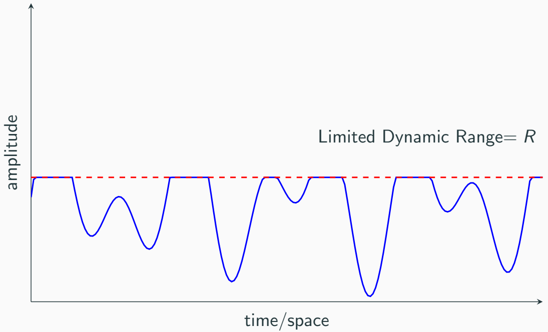

Clipping of the Signal

Solution? $\rightarrow$ Increase the Dynamic Range of the sensor

Expensive

Solution: modulo sensor

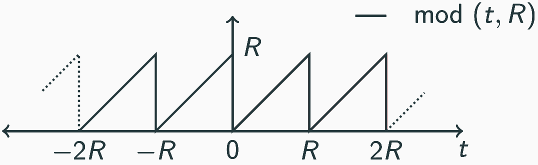

Modulo operation, reminder of $t \div R$

Set-Reset ADC

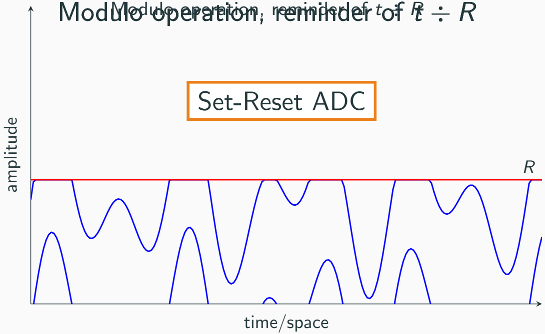

Modulo observations

Modulo image

Challenge: modulo recovery

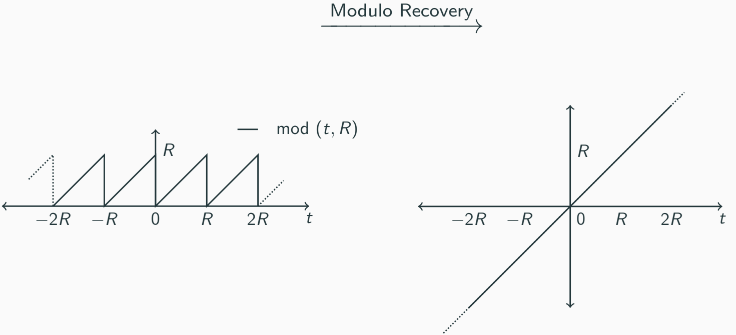

- How to recover the true signal from modulo observations?
- Inverting many-to-one function
- Challenging, ill-posed, non-linear inverse problem

Challenge: modulo recovery

Modulo Recovery

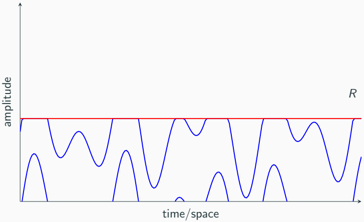

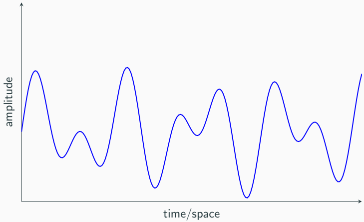

Under certain conditions, recovery is possible.

Modulo Recovery

Prior approaches

Unlimited sampling [1], OLS Method [2], Single-Shot UHDR [8]...

Sampling at sub-Nyquist rate is not possible because:

- Vary only along amplitude dimension
- Follow Nyquist sampling along time dimension
- All rely on bandlimited-ness

To achieve sub-Nyquist sample complexity,

- Bandlimited-ness $\rightarrow$ sparsity
- Vary along both time and amplitude dimension
- Adapt random linear measurements

Our contribution: modulo recovery for compressive sensing

Table 1: Comparison of our approach with existing modulo recovery methods.

	Unlimited Sampling [1]	OLS Method [2]	Multishot UHDR [8]	Our approach
Assumption on structure of signal	bandlimited	bandlimited	no assumptions	**sparsity**
Sampling scheme	uniform grid	uniform grid	(carefully chosen) linear measurements	**random linear measurements**
Sample complexity	oversampled, $\mathcal{O}(n)$	–	oversampled, $\mathcal{O}(n)$	**undersampled,** $\mathcal{O}(s\log(n))$
Provides sample complexity bounds?	Yes	–	No	**Yes**

Our contribution: modulo recovery for compressive sensing

- Signal reconstruction from compressed modulo observations
- Recover $x^* \in \mathbb{R}^n$ using the observations $y \in \mathbb{R}^m$ and the Gaussian random matrix $A = [a_1\ a_2\ \dots\ a_m]^\top \in \mathbb{R}^{m \times n}$.

$$y_i = \mod(\langle a_i \cdot x^* \rangle, R) = \mod(y_{c,i}, R),$$

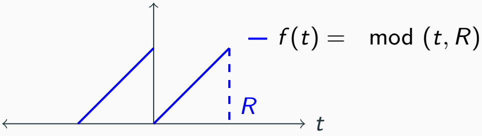

Limit to 2 periods of modulo operation

R is large enough, so all the elements of Ax^* are covered within the domain of operation $[-R, R]$.

still inherits the challenging aspects: non-linearity, many-to-one

Mathematical model

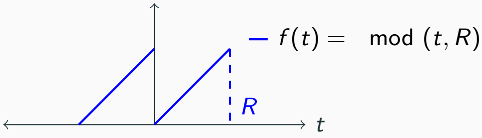

Re-write modulo operation in terms of sgn function,

$$y_i = \langle \mathsf{a_i} \cdot \mathsf{x}^* \rangle + \left(\frac{1 - \mathrm{sgn}(\langle \mathsf{a_i} \cdot \mathsf{x}^* \rangle)}{2} \right) R, \quad i = \{1, .., m\}.$$

$$p_i^* = \frac{1 - \mathrm{sgn}(\langle \mathsf{a_i} \cdot \mathsf{x}^* \rangle)}{2},$$

Bin-index, can be 0 or 1.

The **compressed measurements ($\mathsf{y_c}$)** is equal to $\langle \mathsf{A} \cdot \mathsf{x}^* \rangle$.

$$\mathsf{y_c} = \mathsf{y_i} - \mathsf{p}^* R.$$

MoRAM: basic idea

Inspired by: Jagatap et al., '17 [3]

MoRAM: Modulo Recovery with Alternating Minimization

1. (Carefully) **Initialize** x^0.
    - Calculate the corrected observations and bin-indices $\mathrm{p}^{\mathrm{init}}, \mathrm{y}_{\mathrm{c}}^{\mathrm{init}}$.
    - Calculate the initial estimate using $\mathrm{p}^{\mathrm{init}}$
2. **Alternating Minimization** For $t = 1, 2, ..., T$:
    - Bin-index estimation.
    - Signal estimation.

MoRAM: Initialization

To recover p^* partially:

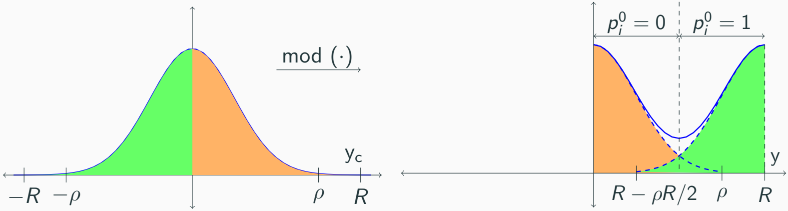

Figure 1: *Density plots of (a)* $\mathrm{y_c} = \mathrm{Ax}^*$*; (b)* $\mathrm{y} = \mod(\mathrm{Ax}^*)$.

- $$p_i^0 = \begin{cases} 0, & \text{if } 0 \leq y_i < R/2 \\ 1, & \text{if } R/2 \leq y_i \leq R \end{cases} \tag{1}$$

MoRAM: Descent through AltMin

Use alternating minimization with Justice Pursuit [4]

- Bin-index estimation: $\mathrm{p}^{\mathrm{t}} = \frac{1-\mathrm{sgn}(\langle \mathrm{A} \cdot \mathrm{x}^{\mathrm{t}} \rangle)}{2}$
- Signal estimation using Justice Pursuit:

$$\mathrm{y}_{\mathrm{c}}^{\mathrm{t}} = \mathrm{y} - \mathrm{p}^{\mathrm{t}} R$$

$$\mathrm{x}^{\mathrm{t}+1} = \underset{\mathrm{u}=[\mathrm{x} \;\; \mathrm{d}]^{\top}}{\arg\min} \|\mathrm{u}\|_1 \; s.t. \; \begin{bmatrix} \mathrm{A} & \mathrm{I} \end{bmatrix} \mathrm{u} = \mathrm{y}_{\mathrm{c}}^{\mathrm{t}}$$

$$\implies \mathrm{x}^{\mathrm{t}+1} = JP(\frac{1}{\sqrt{m}} \begin{bmatrix} \mathrm{A} & \mathrm{I} \end{bmatrix}, \frac{1}{\sqrt{m}} \mathrm{y}_{\mathrm{c}}^{\mathrm{t}}, [\mathrm{x}^{\mathrm{t}} \;\; \mathrm{p}^{\mathrm{t}}]^{\top}).$$

Challenge in signal estimation

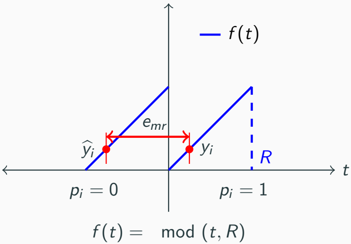

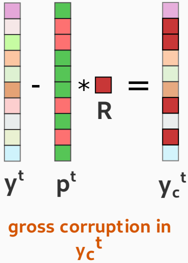

$\boxed{e_{mr} = R}$

Error is constant, additive

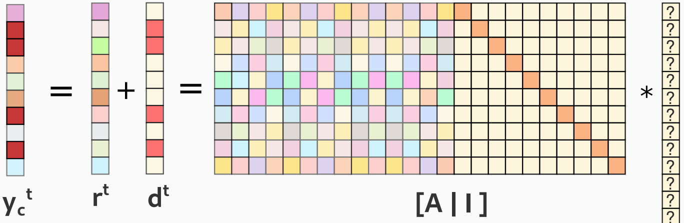

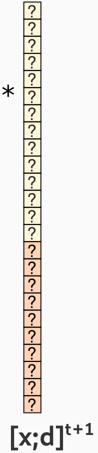

- Error $d^t = p^t - p^*$ is sparse.
- Augmented problem becomes,

$$x^{t+1} = \underset{[x \;\; d]^\top \in \mathcal{M}_{s+s_{d^t}}}{\arg\min} \left\| \begin{bmatrix} A & I \end{bmatrix} \begin{bmatrix} x \\ d \end{bmatrix} - y_c^t \right\|_2^2,$$

- $\boxed{\text{sparsity } s_{d^t} \text{ is unknown} \implies \text{use basis-pursuit formulation}}$

Guarantee: descent

Theorem (Guarantee for descent)

Given $\rho < R$ and the initial estimate of bin-index p^0 obtained using Eq. 1, if the number of modulo measurements m satisfies:

$$m \geq C_1 \left(\|\mathrm{x}^*\|_0 + 2m \frac{\phi(R-\rho)}{(R-\rho)} \right) \log \left(\frac{n+m}{\|\mathrm{x}^*\|_0 + 2m \frac{\phi(R-\rho)}{(R-\rho)}} \right),$$

then the first iteration of Algorithm 2 returns the true signal x^0 with probability exceeding $1 - 3e^{-C_2 m}$, where C_1 and C_2 are constants that depend only on the RIP constants for the augmented measurement matrix $[\mathrm{A} \quad \mathrm{I}]$.

$\boxed{\text{Sample complexity: } \mathcal{O}(s \log n)}$

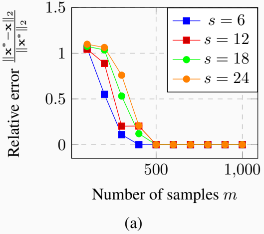

Figure 2: Mean relative reconstruction error vs no. of measurements (m) for MoRAM with $\|x^*\|_2 = 1, n = 1000$, and (a) $R = 3.2$; (b) $R = 3.6$.

Experiments with real images

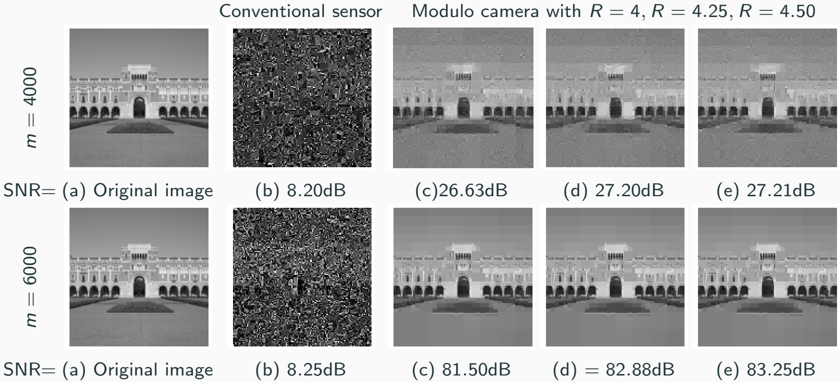

Figure 3: Sparse reconstructions ($s = 800$) of original Lovett Hall image ($n = 16,384$); with $m = 4000$ and $m = 6000$ measurements (b) using basis pursuit for observations from a conventional sensor with dynamic range $[0, 4]$; (c,d,e) using MoRAM for modulo observations obtained with modulo sensor with dynamic range $[0, R]$ with $R = 4, 4.25, 4.5$.

Summary and future work

Summary:

- Novel problem of modulo recovery with compressive sensing
- Provable algorithm, leverages sparsity
- $\mathcal{O}(s \log n)$ sample complexity

Future directions:

- Extend to noisy observations
- Extend beyond 2 periods
- Explore generative priors

Summary of other research

- V. Shah and M.Soltani and C. Hegde,
  Reconstruction from Periodic Nonlinearities, with Applications to HDR Imaging,
  Asilomar Conference on Signals, Systems, and Computers, November 2017.
- V. Shah and C. Hegde,
  Solving Linear Inverse Problems using GAN Priors: an Algorithm with Provable Guarantees,
  International Conference on Acoustics, Speech, and Signal Processing, 2018.
- In collaboration with R. Singh and B. Pokuri and C. Hegde and S. Sarkar and B. Ganapathysubramanian
  Physics-aware Deep Generative Models for Creating Synthetic Microstructures,
  to be submitted to: *Machine Learning for Molecules and Materials Workshop at Neural Information Processing Systems, 2018.*
- R. Hyder and V. Shah and C. Hegde and S. Asif,
  Alternating Phase Projected Gradient Descent with Generative Priors for Solving Compressive Phase Retrieval,
  submitted to: *International Conference on Acoustics, Speech, and Signal Processing, 2019.*

Summary and future work

Summary:

- Novel problem of modulo recovery with compressive sensing
- Provable algorithm, leverages sparsity
- $\mathcal{O}(s \log n)$ sample complexity

Future directions:

- Extend to noisy observations
- Extend beyond 2 periods
- Explore generative priors

A. Bhandari, F. Krahmer, and R. Raskar.
On unlimited sampling.
Proc. Sampling Theory and Applications (SampTA), pages 31–35, 2017.

M. Cucuringu and H. Tyagi.
On denoising modulo 1 samples of a function.
In *Proc. Int. Conf. Art. Intell. Stat. (AISTATS)*, 2018.

G. Jagatap and C. Hegde.
Fast, sample-efficient algorithms for structured phase retrieval.
In *Proc. Adv. in Neural Inf. Proc. Sys. (NIPS)*, 2017.

J. Laska, M. Davenport, and R. Baraniuk.
Exact signal recovery from sparsely corrupted measurements through the pursuit of justice.
In *Proc. Asilomar Conf. Signals, Systems, and Computers*, pages 1556–1560, 2009.

V. Shah and C. Hegde.
Solving linear inverse problems using gan priors: An algorithm with provable guarantees.
Proc. IEEE Int. Conf. Acoust., Speech, and Signal Processing (ICASSP), 2018.

- V. Shah, M. Soltani, and C. Hegde.
  Reconstruction from periodic nonlinearities, with applications to hdr imaging.
  In *Proc. Asilomar Conf. Signals, Systems, and Computers*, pages 863–867. IEEE, 2017.
- R. Vershynin.
  Introduction to the non-ptotic analysis of random matrices.
  arXiv preprint arXiv:1011.3027, 2010.
- H. Zhao, B. Shi, C. Fernandez-Cull, S. Yeung, and R. Raskar.
  Unbounded high dynamic range photography using a modulo camera.
  In *Intl. Conf. on Comp. Photography (ICCP)*, 2015.

Ideas from the sparse phase retrieval

- Phase retrieval: we are given observations of the form:

$$y_i = |\langle \mathrm{a_i}, \mathrm{x}^* \rangle|, \quad i = 1, 2, \ldots, m,$$

and are tasked with reconstructing x^*.

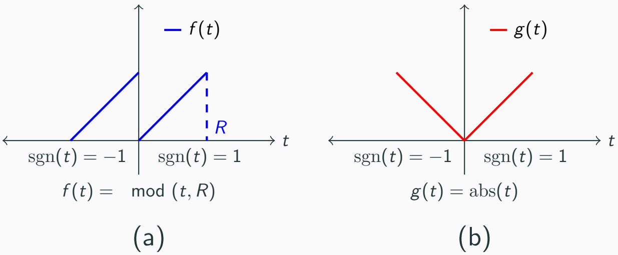

Figure 4: *Comparison between (a) modulo function ($f(t) = \mod(t, R)$); and (b) absolute value function ($g(t) = \mathrm{abs}(t)$).*

$\boxed{\text{Striking similarities}}$

Initialization

A hyper-parameter ρ approximates the $l\infty-$norm of Ax^*.

1. Calculate corrected observations y_c.
   - Calculate p^{init} as:

$$p_i^{init} = \begin{cases} 0, & \text{if } 0 \leq y_i < (R - \rho) \quad \text{(set } Y_+\text{)} \\ 0, & \text{if } (R - \rho) \leq y_i < \rho \quad \text{(region of uncertainty)} \\ 1, & \text{if } \rho \leq y_i < R \quad \text{(set } Y_-\text{)} \end{cases}$$

   - Calculate y_c^{init}:

$$y_c^{init} = y + p^{init} R.$$

   - set $U = Y_+ \cup Y_-$, $N = \mathrm{card}(U)$.
2. Calculate initial estimate x^0

$$x^0 = H_s \left(\frac{1}{N} \sum_{i=1}^{N} y_{c,U,i}^{init} a_{U,i} \right), \tag{2}$$

where H_s denotes the hard thresholding operator.

Initialization

Algorithm 1 MoRAM-initialization

Inputs: y, A, s, R, ρ

Output: x^0

$U \leftarrow \emptyset$

for $i = 0 : m$ **do**

  if $(R - \rho) > y_i$ or $y_i \geq \rho$ **then**

    $U \leftarrow U \cup \{i\}$

  end if

  Calculate p_i^{init} according to Eq. 1.

end for

$N \leftarrow |U|$, calculate $\mathrm{y}_\mathrm{c}^{\mathrm{init}}$ according to Eq. **??**

$\mathrm{x}^0 \leftarrow H_s\left(\frac{1}{N}\sum_{i=1}^{N} y_{c,U,i}^{init} a_{U,i}\right)$

Signal estimation with Justice pursuit

Algorithm 2 MoRAM-descent

Inputs: y, A, s, R

Output: x^{T}

$m, n \leftarrow \mathrm{size}(\mathsf{A})$

Initialization

$\mathsf{x}^0 \leftarrow \mathrm{MoRAM\text{-}initialization}(\mathsf{y}, \mathsf{A})$

Alternating Minimization

for $t = 0 : T$ **do**

$\quad \mathsf{p}^{\mathsf{t}} \leftarrow \frac{1-\mathrm{sgn}(\langle \mathsf{A}\cdot\mathsf{x}^{\mathsf{t}}\rangle)}{2}$

$\quad \mathsf{y}_{\mathsf{c}}^{\mathsf{t}} \leftarrow \mathsf{y} - \mathsf{p}^{\mathsf{t}} R$

$\quad \mathsf{x}^{\mathsf{t+1}} \leftarrow JP(\frac{1}{\sqrt{m}}\begin{bmatrix}\mathsf{A} & \mathsf{I}\end{bmatrix}, \frac{1}{\sqrt{m}}\mathsf{y}_{\mathsf{c}}^{\mathsf{t}}, [\mathsf{x}^{\mathsf{t}} \quad \mathsf{p}^{\mathsf{t}}]^{\top}).$

end for

Differences between phase retrieval and modulo recovery

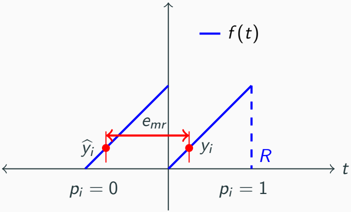

$f(t) = \mod(t, R)$

$$\boxed{e_{mr} = R}$$

Error is constant, additive

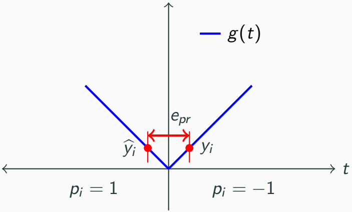

$g(t) = \mathrm{abs}(t)$

$$\boxed{e_{pr} = 2|y_i|}$$

Error is linear w.r.t. y_i

The challenge in signal estimation step

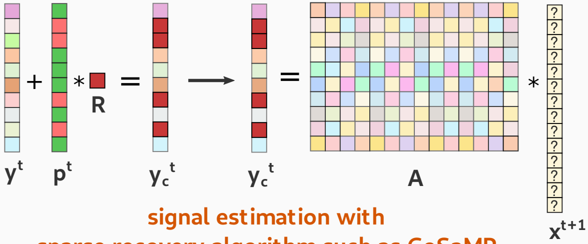

signal estimation with
sparse recovery algorithm such as CoSaMP

$$y_c^t = \langle A x^t \rangle = y - p^t R,$$

$$x^{t+1} = \arg\min_{x \in \mathcal{M}_s} \|Ax - y_c^t\|_2^2,$$

$$\implies x^{t+1} = \mathrm{CoSaMP}\left(\frac{1}{\sqrt{m}} A, \frac{1}{\sqrt{m}} y_c^t, s, x^t\right).$$

$\boxed{\text{if } |e_{y_i}| \leq \epsilon \implies |e_{x^{t+1}}| \leq C\epsilon.}$ Here, $\epsilon = R$.

Justice Pursuit

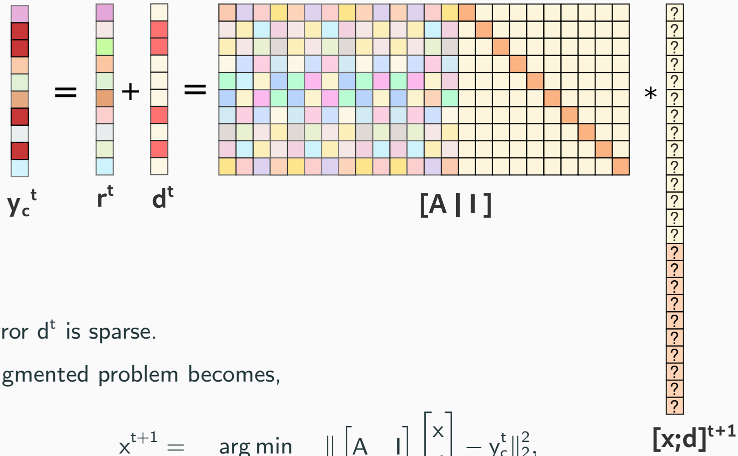

- Error d^t is sparse.
- augmented problem becomes,

$$x^{t+1} = \underset{[x \;\; d]^\top \in \mathcal{M}_{s+s_{d^t}}}{\arg\min} \left\| \begin{bmatrix} A & I \end{bmatrix} \begin{bmatrix} x \\ d \end{bmatrix} - y_c^t \right\|_2^2,$$

- $\boxed{\text{sparsity } s_{d^t} \text{ is unknown } \implies \text{ use basis-pursuit formulation}}$

Proof sketch

Proof sketch: Initialization

- Establish lower bound on N
  - $N \geq m\left(1 - 2\frac{\phi(R-\rho)}{(R-\rho)}\right)$.
- Bound $\|x^* - \widehat{x}^0\|$ where, $x^0 = H_s\left(\widehat{x}^0\right)$.
- Establish the result with the union bound over all the $s-$sparse vectors.

Proof sketch: Descent

- Theoretically, only 1 signal estimation with of JP is needed ($T = 1$).
- Show that the mapping $F(x) := \mathrm{sgn}(Ax)$ is Binary ϵ-Stable Embedding.
- Establish x^0 and x^* are $\delta-$ close $\implies \|d^0\|_0 = \|(p^* - p^0)R\|_0 \leq \gamma m$.
- Use the fact that $x^1 = x^*$ if $\|d^0\|_0 \leq \gamma m$ with γ being positive fraction.

Proof sketch: initialization

$$\tilde{x}^0 = M = \frac{1}{N} A_T^\top A_T x^*.$$

Each row of our truncated Gaussian measurement matrix ($A_{U\times S}$) is independent, and also follows the Gaussian distribution with zero mean. We denote this distribution with Gaussian random vector Z in $\mathbb{R}^s$, and arrange N rows as the independent samples from the distribution; $Z_i := A_{U\times S,i}$. The covariance matrix of Z can be calculated as $\Sigma = \mathbb{E}Z \otimes Z$,

$$\Sigma = \mathbb{E}Z \otimes Z = \mathbb{E}ZZ^\top = \text{diag}(\mathbb{E}z_1^2, \mathbb{E}z_2^2, \ldots, \mathbb{E}z_n^2) = I_n.$$

Now, calculate the sample covariance matrix of Z using the samples $Z_i = A_{\times S,i}$,

$$\Sigma_N = \frac{1}{N}\sum_{i=1}^{N} Z_i \otimes Z_i = \frac{1}{N} A_{U\times S}^\top A_{U\times S}.$$

Given $N \geq C\left(\frac{t}{\kappa}\right)^2 s$, we invoke the Corollary 5.50 of [7] which relates Σ_N and Σ as following with probability at least $1 - 2\exp\left(-t^2 s\right)$:

$$\begin{aligned} \|\Sigma_N - \Sigma\| &\leq \kappa \\ \implies \|\frac{1}{N} A_{U\times S}^\top A_{U\times S} - I_s\| &\leq \kappa \end{aligned}$$

Mathematical analysis

Here, let us fix the $s-$sparse vector x^* in unit norm ball. We can evaluate the operator norm in above equation over set of $s-$sparse vectors in unit norm ball.

$$\implies \sup_{x \in S} \frac{\| \left(\frac{1}{N} A_{U \times S}^{\top} A_{U \times S} - I_n \right) x \|_2}{\|x\|_2} \leq \kappa$$

$$\| \left(\frac{1}{N} A_{U \times S}^{\top} A_{U \times S} x^* - x^* \right) \|_2 \leq \kappa \|x^*{}_2\|$$

$$\|\tilde{x}^0 - x^* \|_2 \leq \kappa \|x^* \|_2$$

with probability at least $1 - 2\exp\left(-t^2 s\right)$ given the fixed $s-$sparse vector x^*. Take union bound over all $\binom{n}{s}$ such $s-$sparse vectors.

Binary ϵ-Stable Embedding

A mapping $F : \mathbb{R}^n \to \mathcal{B}^m$ is a binary ϵ-stable embedding (BϵSE) of order s for sparse vectors if:

$$d_S(x, y) - \epsilon \leq d_H(F(x), F(y)) \leq d_S(x, y) + \epsilon;$$

for all $x, y \in S^{n-1}$ with $|supp(x) \cup supp(y)| \leq s$.

Reconstruction from Periodic Non-linearities [6], Spring 2017

V. Shah and M.Soltani and C. Hegde,

Reconstruction from Periodic Nonlinearities, with Applications to HDR Imaging,

Asilomar Conference on Signals, Systems, and Computers, November 2017.

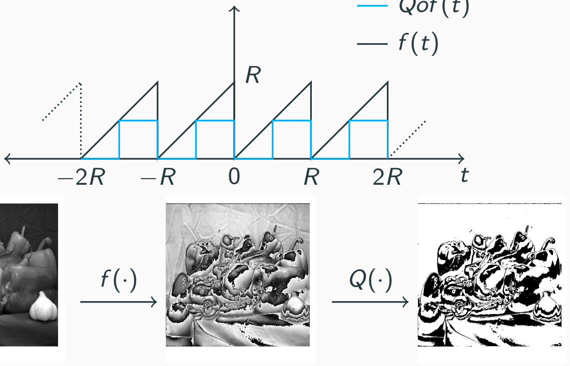

Reconstruction from Periodic Non-linearities [6]

Our Algorithm: RQM-Recovery from Quantized Modulo images

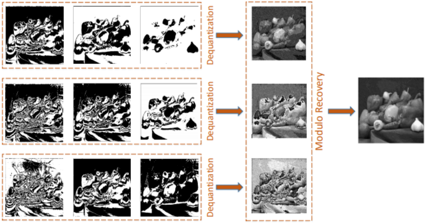

Stagewise approach

- **Dequantization**: Recover u from $y = Q(Cu)$ using HM algorithm.
- **Modulo recovery**: Recover z from $u = f(Dx)$ using MF-Sparse [2] or Multi-shot UHDR [1].
- **Sparse recovery**: Recover x from $z = Bx$ using any stable sparse recovery algorithm (e.g. CoSaMP).

Algorithm:RQM

Inputs: $y, D, B, C, k, k', \Omega, s$
Output: $\widehat{x}$
Stage 1: Harmonic dequantization
$\widehat{u} \leftarrow \text{HMDEQUANTIZATION}(y, C, k)$
Stage 2: Modulo recovery[2]
$\theta \leftarrow \exp(i\widehat{u})$
for $l = 1 : q$ **do**
  $t \leftarrow D(l : q : (k'-1)q + l, l)$
  $\phi \leftarrow \theta(l : q : (k'-1)q + l)$
  $\widehat{z}_l = \text{argmax}_{\omega \in \Omega} |\langle y, \psi_\omega \rangle|$
end for
$\widehat{z} \leftarrow [\widehat{z}_1, \widehat{z}_2 \ldots, \widehat{z}_q]^T$
Stage 3: Sparse recovery
$\widehat{x} \leftarrow \text{COSAMP}(\widehat{z}, B, s)$

Experimental Results

Recovery from Quantized Modulo images

without sparsity

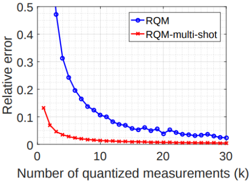

with sparsity

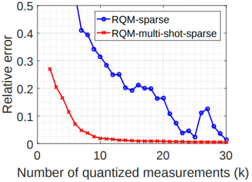

Solving Linear Inverse Problems using GAN Priors [5], Fall 2017

V. Shah and C. Hegde,

Solving Linear Inverse Problems using GAN Priors: an Algorithm with Provable Guarantees,

International Conference on Acoustics, Speech, and Signal Processing, 2018.

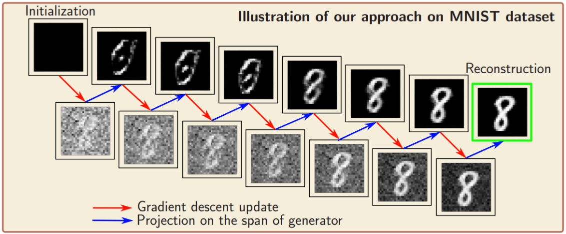

Solving Linear Inverse Problems using GAN Priors [5]

- We train the generator $G : \mathbb{R}^k \to \mathbb{R}^n$:

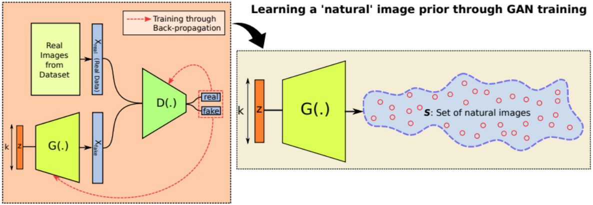

- With pre-trained generator(G), apply Projected Gradient Descent in 2 steps:

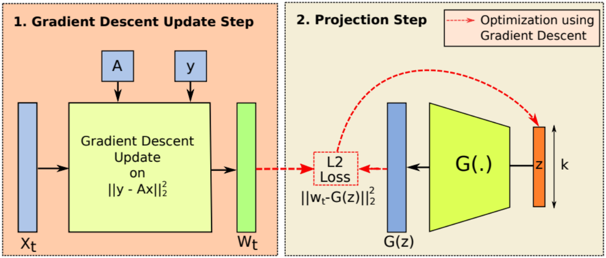

Solving Linear Inverse Problems using GAN Priors [5]

Experimental Results

on MNIST dataset

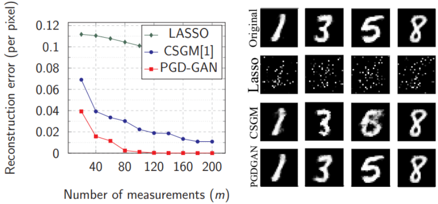

on celebA dataset

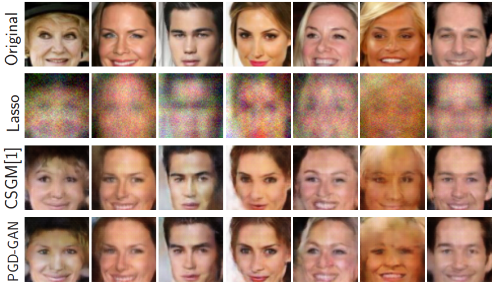

Physics-aware Deep Generative Models, Fall 2018

In collaboration with R. Singh and B. Pokuri and C. Hegde and S. Sarkar and B. Ganapathysubramanian

Physics-aware Deep Generative Models for Creating Synthetic Microstructures, to be submitted to: Machine Learning for Molecules and Materials Workshop at Neural Information Processing Systems, 2018.

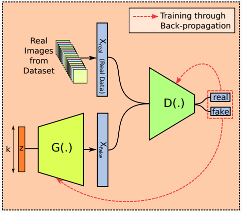

(a)

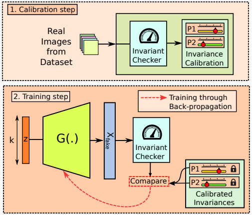

(b)

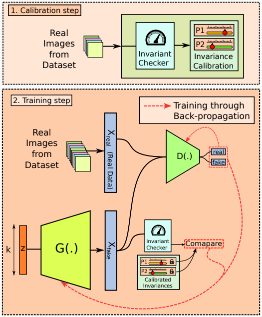

(c)

Figure 5: (a) Generative Adversarial Network model; (b) Generative Invariant Network model; (c) Hybrid (GAN+GIN) model.

Physics-aware Deep Generative Models

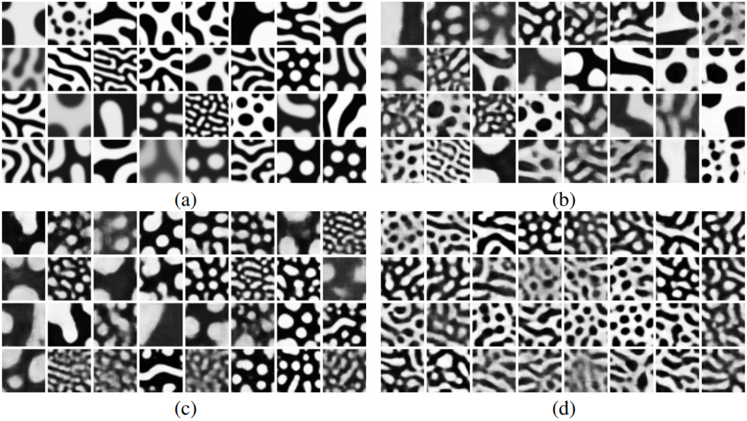

Figure 3: (a) Sample images from Cahn-Hilliard dataset; (b) samples generated by WGAN-GP trained on CH-dataset; (c) Samples generated by WGAN-GP trained over the morphologies from CH_{p1} dataset (only includes the images with volume fraction between 0.35 to 0.45); (d) Samples generated by WGAN-GP trained over the morphologies from CH_{p2} dataset (only includes the images with 2−point correlation equal to 0.0625).

Physics-aware Deep Generative Models

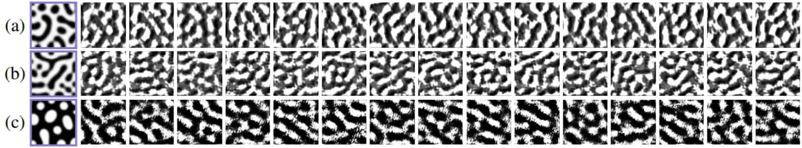

Figure 8: Images generated by GIN models; with first image in each row being the real image used for calibration. (a,b) are trained over enite p_2 curve while model in (c) used only the initial portion of p_2 curve.

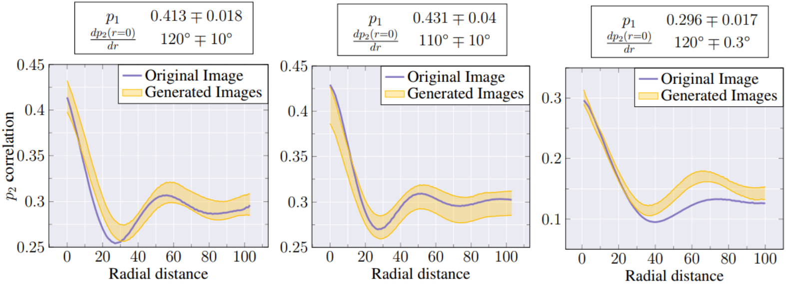

(a) GIN trained on entire p_2 curve (b) GIN trained on entire p_2 curve (c) GIN trained on initial portion of p_2 curve

Physics-aware Deep Generative Models

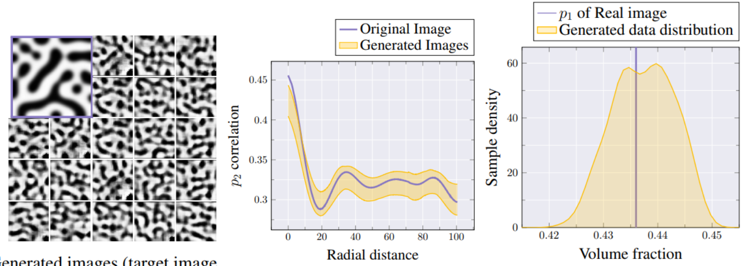

(a) Generated images (target image on top right)

(b) 2−point correlation curves

(c) Distribution of p_1

Figure 10: Comparisons of volume fraction (p_1) distribution and 2− point correlation curves between the images generated by hybrid GAN and the target image.

Phase retrieval using generative priors, Fall 2018

R. Hyder and V. Shah and C. Hegde and S. Asif,
Alternating Phase Projected Gradient Descent with Generative Priors for Solving Compressive Phase Retrieval,
submitted to: International Conference on Acoustics, Speech, and Signal Processing, 2019.